Springer

Journal of Mechanical Science and Technology 23 (2009) 1270~1277

Journal of Mechanical Science and Technology

www.springerlink.com/content/1738-494x
DOI 10.1007/s12206-008-1202-2

Effect of imperfections on the mechanical behavior of wire-woven bulk kagome truss PCMs under shear loading †

Sangil Hyun[1], Ji-Eun Choi [2], and Ki-Ju Kang[3,*]

[1]*Simulation Center, Korea Inst. of Ceramic Eng. & Tech., Seoul, Korea*
[2]*Automobile Research Center, Chonnam National University, Gwangju, Korea*
[3]*School of Mechanical Systems Engineering, Chonnam National University, Gwangju, Korea*

(Manuscript Received April 10, 2008; Revised September 30, 2008; Accepted December 5, 2008)

Abstract

Wire-woven bulk kagome (WBK) materials are a new class of cellular metallic structures possessing desired mechanical performance and can be fabricated easily by assembling metallic wires. In previous studies, the WBK materials were shown to have high strength and weak sensitivity on imperfections under compressive loads. In this paper, we present numerical simulation results on the mechanical performance of WBK and its sensitivity on imperfections under shear loads. Two types of statistical imperfections on geometry and material property were introduced in the simulation models as likewise the previous studies. The simulation results were compared with the experimental measurement on the WBK made of stainless wire (SUS304). The WBK were shown to have a good isotropic mechanical strength under various orientations of shear loadings.

Keywords: Cellular metal; PCM (Periodic Cellular Metal); Kagome truss; Imperfections; PBC (periodic boundary condition); Random network analysis

1. Introduction

A new type of periodic cellular metal (PCM) termed kagome truss[1] has gained considerable attention for its superior mechanical, electrical, thermal performance than any other type of PCMs [2-7]. The mass production method has been intensively studied for its potential applications, and a variety of fabrication techniques have been suggested in many studies. Among them, a new-type of fabrication technique using wires (WBK) [8] was recently suggested by one of the authors [9]. In the WBK technique, continuous helical wires are systematically assembled in six different directions based on the kagome lattice structures [10]. Due to the ease of construction with helical wires, this fabrication process has demonstrated a strong possibility for the mass production of robust kagome truss cores [11]. In addition, the strength and stiffness of WBK can be easily improved by specific heat treatment after the assembling process.

Analytic predictions of the mechanical behaviors of bulk periodic cellular metals, however, have been considered extremely difficult due to the possible imperfections in realistic models such as irregular wire windings and defects at brazed joints. Thus, numerical approaches are generally employed to predict the mechanical properties of the WBK, such as elastic coefficient and strengths, in a systematic manner. Due to the huge number of cells composing a WBK, effective simulation techniques have been sought to minimize the computational effort. In our previous studies [12, 13], a new simulation approach using finite element method and random network analysis was developed to investigate the mechanical performance of WBK under compressive loads. In the studies, the finite element method was employed for the analysis on a sin-

† This paper was recommended for publication in revised form by Associate Editor Maenghyo Cho

* Corresponding author. Tel.: +82 62 530 1668, Fax.: +82 62 530 1689
E-mail address: kjkang@chonnam.ac.kr

gle unit cell under periodic boundary conditions, which allowed us to determine the elastic and plastic behavior of single WBK truss. By utilizing the material properties of single truss obtained from the finite element analysis, the random network analysis was performed to analyze the effect of imperfections on the mechanical behavior. The generic form of the random network analysis [14, 15] has been widely used to analyze a variety of characteristics (e.g., mechanical, electrical, thermal) for various lattice structures consisting of a spring or truss.

To simulate the imperfections in realistic truss structures, we considered two types of feasible defects as introduced in the previous studies [12, 13]. One was geometric defects corresponding to the deviation of the joints from the ideal lattice points. The other was material property defects corresponding to the irregularities generated at the brazed joints or truss elements. We introduced these types of imperfections in the ideal WBK structures in a statistical manner following Gaussian distribution functions.

In the current study, the mechanical behavior of the WBK models subjected to shear loads has been analyzed in a wide range of imperfection levels. The isotropic characteristics of the WBK were also examined in three selected shear orientations. The numerical results were validated by being compared to the result of experimental measurement in a specific orientation.

2. The topology and preparation of the specimen

The idea of the wire-woven bulk kagome (WBK) stems from a two-dimensional kagome structure which is assembled simply by tri-axial weaving of wires, as shown in Fig. 1(a). To construct a 3-dimensional version of the structure, a pair of triangles indicated by the solid line and the parallelogram indicated by the dotted line in Fig. 1(a) should be converted into a pair of tetrahedrons and a parallelepiped, as shown in Figs. 1(b) and 1(c), respectively. Consequently, the three-dimensional version of the structure shown in Fig. 1(a) would be a structure like that shown in Fig. 1(d), which is composed of parallel wire groups in six directions. Of the parallel wire groups in six directions, three groups are in-plane and the remaining three groups are out-of-plane. The wires cross each other at an angle of 60° or 120°. The pair of tetrahedrons or a parallelepiped shown in Fig.1 (b) or (c), respectively, is a unit cell of WBK.

To investigate the orientation dependency of the

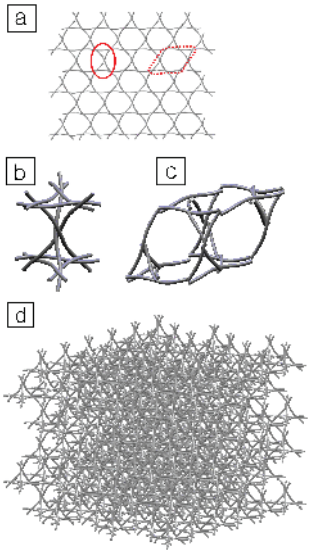

Fig. 1. Configurations of (a) two-dimensional kagome truss woven by three directional wires, in which the triangles surrounded by the solid line and the parallelogram surrounded by the dashed line are, respectively, converted into (b) tetrahedrons and (c) parallelepiped in (d) the three-dimensional kagome truss woven by six directional wires (WBK).

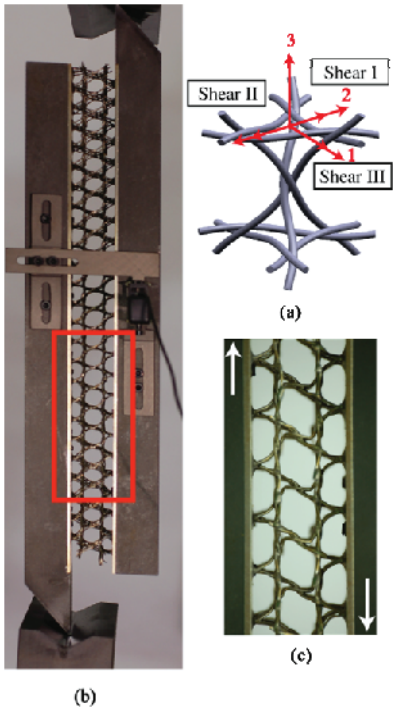

Fig. 2. (a) Definitions of shear load directions, (b) a picture of the WBK specimens with a pair of shear test jigs mounted to material test system, and (c) the enlarged view of deformation of the WBK specimen after the test.

shear strength, finite displacements in three different directions were applied on the unit cell of the WBK as shown in Fig. 2(a). These are positive (orientation I) and negative (orientation II) directions in the 2 axis and positive (orientation III) direction in the 1 axis. The experimental shear test shown in Figs. 2(b) and 2(c) was performed in the orientation I according to the ASTM standard (ASTM C273) [16]. The test specimen has 25 unit cells in length, 3 unit cells in width. The SUS304 stainless steel WBK cores were assembled and then brazed with Nicrobraz®LM (BNI-2 paste, Wall Colmonoy Corp.) pastes in all the closing point of the wires. The pitch of the helix was P = 16.2 *mm*, the helical radius was A = 0.46 *mm*, and the wire radius was R = 0.78 *mm*.

3. The definition of imperfections and simulation models

Each truss element in the network model is modeled by the stainless wire (SUS304) of the same size with the real WBK strut (see Fig. 2). A typical network model consisting of 6 unit cells both in the planar directions (*x* and *y*) and 5 unit cells in the normal direction (*z*) was used in the simulation. The number of nodes and truss elements was 828 and 2177, respectively. To remove the boundary effect under the planar deformation, periodic boundary conditions were imposed in the *x*-*y* directions. The simulation was first performed with a perfect lattice model without any imperfection, and the result was compared with the experimental result in a specific orientation (I). Later, the simulations were performed on the models with geometric imperfections and material imperfections in the three shear orientations.

3.1 Periodic boundary conditions (PBC)

When a structure consisting of many uniform cells like WBK is to be analyzed, numerical analysis for the whole structural system can be severely inefficient or even impossible. An alternative is to use the periodicity of the structure expressed by periodic boundary condition. Mills [17] successfully simulated large compressive deformations of an open cell foam by applying the 3-dimensional periodic boundary condition to a representative unit cell with multi point constraint (MPC) coded in a commercial software ABAQUS.

In a truss PCM, a constant unit cell is repeated in three-dimensional space to construct a bulk structure. Figs. 1(b) and (c) show the configurations of two different unit cells of WBK. In the macroscopic viewpoint, WBK can be regarded as a bulk material. If a sample of WBK is composed of an infinite number of unit cells, the effect of the outer surfaces on the bulk material properties can be ignored and the mechanical behavior can be estimated by analyzing the inner material. Suppose that all the cells in the inner material deform uniformly under the external force acting on the bulk sample. The deformation of the cells should be compatible with each other, namely, the deformed shape of a unit cell must be matched with that of the neighbors.

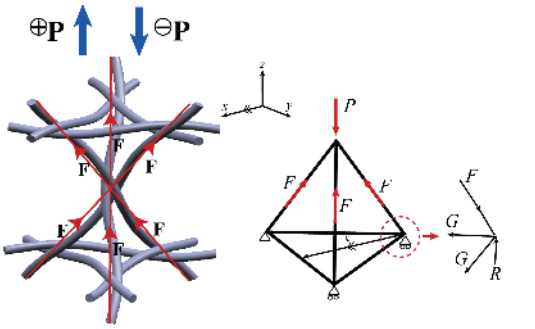

Fig. 3. The configuration of (a) a unit cell under compression and tension, and (b)an idealized form of the lower tetrahedron.

To apply the periodic boundary condition on the unit cell of WBK in the finite element analysis, the following scheme was used. Eq. (1) expresses the constraint equations of the unit cells as the periodic boundary conditions.

$$\begin{aligned} u_1|_j - u_1|_{j'} &= u_1(C_o) \\ u_2|_j - u_2|_{j'} &= u_2(C_o) \qquad (j, j' = 1,2,...,n) \\ u_3|_j - u_3|_{j'} &= u_3(C_o) \end{aligned} \tag{1}$$

where u_1, u_2, u_3 and Co denote the displacements in the *x*, *y* and *z* directions and the reference point, respectively. The subscript, *j*, denotes the nodes on the upper surface, while *j*' denotes the corresponding nodes on the lower surface. Every pair of nodes denoted by j and j' is displaced with a constant difference $u_i(C_o)$ (i=1, 2, 3) in the *x*, *y* and *z* directions.

3.2 Estimation of force-displacement relation of a single strut

The perfect lattice model consists of all equal-size truss elements and all nodes at precise kagome lattice points. To model the nonlinear property of a realistic elasto-plastic strut, finite element analysis was performed on the unit cell model of WBK. The result of finite element simulation was used to construct the force-displacement curve of a single strut following the conversion procedure. Since either tensile or compressive reaction force can be applied in the struts under shear loads, two separate force-displacement relations are required for both tensile and compressive loads.

Fig. 3(a) shows the external loads and the reaction forces in the unit cell used in the finite element analysis. First, a compressive or tensile load, P, was applied to the unit cell model, and the displacement, δ_P, was generated in the normal direction. The result of the unit cell was used to estimate the force-displacement relation of a single strut on the basis of the argument as follows [12]: Fig. 3(b) shows the lower regular tetrahedron truss of idealized form of the unit cell of Fig. 3(a). The equilibrium of forces leads to the relations $P=\sqrt{6}F$ and $G=\frac{F}{3}$. Consequently, the elastic energy can be expressed as

$$U=3U_F+3U_G=\frac{5P^2}{18k} \tag{2}$$

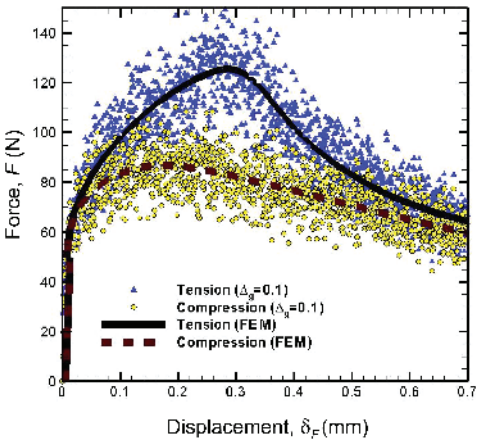

Fig. 4. Force vs. displacement curves (in tension and compression) with Gaussian defects (Δ_p) obtained by FEM on a unit cell. The symbols of circle and delta represent possible distributions of the curves when the Gaussian defects (Δ_p= 0.1) are considered.

where the strength of the truss element k can be expressed as $k=\frac{\pi Ed^2}{4a}$. According to Castigliano's second theorem, the displacement generated in the whole unit cell can be expressed as

$$\delta_P=2\times\frac{5P}{9k}=\frac{40aP}{9\pi Ed^2} \tag{3}$$

The deformation of one unit cell can be expressed as

$$\delta_F=\frac{F}{k}=\frac{4aF}{\pi Ed^2} \tag{4}$$

Because $P=\sqrt{6}F$, the relation between δ_F and δ_P can be given by

$$\delta_F=\frac{9\delta_p}{10\sqrt{6}} \tag{5}$$

Then, the force-displacement relation of the single strut F vs. δ_F can be determined from the relation of P vs. δ_P. Fig. 4 shows the two curves of F vs. δ_F, obtained for the struts under tensile (solid) and compressive (dotted) forces. To cover the wide range of displacement, we interpolated and extrapolated the curves of F vs. δ_F by using 6th order polynomials in Eq. (6).

$$F(\delta_F)=\sum_{i=0}^{6}C_i{\delta_F}^i \tag{6}$$

where C_i are the fitting coefficients. The fittings were done in three separate regions for each curve. The fitted curves were used to model the nonlinear characteristics of each strut in the network models.

3.3 Definition of imperfections

To simulate the realistic models, we introduced two types of imperfections to the perfect lattice model: geometric imperfection and material property imperfection. The distributions of both imperfections were prescribed in the form of Gaussian functions. To achieve good statistics for the random network analysis, we generated a reasonable size (828 nodes and 2177 trusses) of truss models including random defects. We present a typical geometry of the network simulation model used in the network analysis. Fig. 5(a) shows the initial (red) and deformed (green) ge-

ometry of a perfect network model, and Fig. 5(b) shows another deformation model with geometric imperfections.

The distribution of the normalized truss length (dr/a) of a defect model with geometric imperfections ($a = 8.1mm$) is defined by

$$\vec{x} = \vec{x}_0 + a\vec{\Delta}_g \tag{7}$$

Fig. 6 shows the distribution of truss length of the imperfection models ($\Delta_g = 0$ and 0.1) before and after the shear deformation. Note the distribution of perfect lattice model has single peak at $dr/a = 1$.

The distribution for the geometrical defects before the deformation shows a single sharp peak at $dr/a = 1$ with a Gaussian width. After the deformation, however, a wide distribution of truss length can be observed around the initial peak. It is shown that some struts are stretched, while some others are compressed under the shear deformations.

Another type of imperfection of material property is introduced. Since some imperfect shapes (e.g., curvature) and defects can be included in the struts and joints during the manufacturing process, it is reasonable to expect an inhomogeneous modulus of the struts. To model this type of imperfection, we added random variations on the force (F) vs. displacement (d) curves (see Fig. 4). We prescribed the standard deviation (Δ_p) of the Gaussian distributions and added it to the curve by the following equation:

$$F(d) = F_0(d)(1 + \Delta_p) \tag{8}$$

In Fig. 4, the compressive and tensile response curves of the perfect truss model were transformed to cover the wide regions (triangular and circular points) by introducing the material property imperfections with Gaussian distributions.

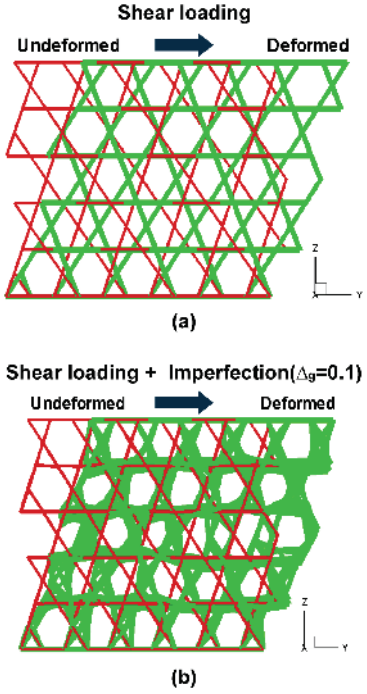

Fig. 5. Geometry of random network models under shear loadings: (a) a perfect network model without imperfection, and (b) a network model with geometrical imperfections(Δ_g =0.1).

4. The effects of imperfections

Fig. 7 presents the stress/strain curves of the perfect WBK core under the three shear deformations (see Fig. 2(a)). The experimental result measured on a specimen under the shear orientation I was added for a comparison. The figure shows similar responses in all three orientations before reaching the maximum stress points. Namely, all the cores yield at a stress ($\tau = 0.08$) followed by strain hardening.

The maximum stress in orientation I is given by τ_{max}=0.18, which is 11% higher than that of orientation III, and the maximum strain in orientation I is given by $\gamma_{\max} = 0.13$. By comparing with the experiment, the simulation result slightly overestimates the peak load (possibly due to the open boundary and the imperfections of the experimental specimen), but in the overall behavior it captures all aspects of the shear stress/strain curves.

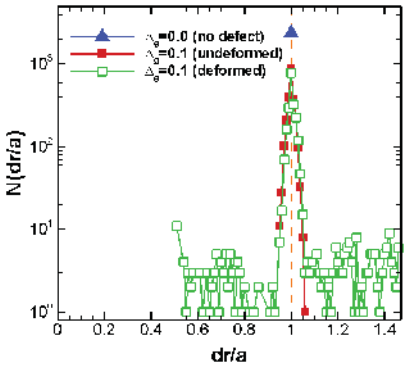

Fig. 6. The distributions of normalized truss length for WBK truss model before and after the shear loadings.

We examined the dependence of the strength on the imperfections of geometry and material property for the imperfection level from 0 to 0.2. The stress/strain curves for the specified imperfections under shear orientation I, II, III are summarized in Fig. 8. Both imperfections of geometry and material property minimally affect the mechanical behaviors of the WBK before the maximum stress. The numerical result (a) and (b) in the orientation I is compared with the experimental result. The defect model with some degree of imperfection can show better agreement with the experimental result. It is suspected that the actual specimen may possess some types of defects generated in the fabrication process. In the other shear directions (II, III), the figures (c)~(f) show that the peak stress stays nearly unchanged up to a certain strain, dropping significantly afterward. In addition, orientation II shows faster drops beyond the maximum stress than the other orientations I and III. We noted that the stress drop after the peak stress could be more severe for tensile load than compressive load (see Fig. 4).

Thus, this fast stress drop in orientation II is partially due to the pure tensile load applied on one strut in the tripod. Note that none of trusses is not under pure tensile load in other orientations. In addition, the stress drop for the defect free cases is also significant, in which all of the trusses yield same time after the yield. Nevertheless, in the post yield regime, all of the stresses tend to approach to certain values independently on the defect levels. In addition, the WBK structures with defects were found slightly more robust to the imperfections in orientation I than the other orien-

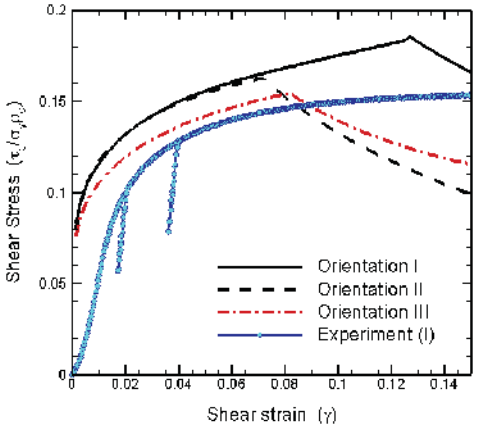

Fig. 7. Stress vs strain curves of the perfect WBK in three shear deformations and an experimental result.

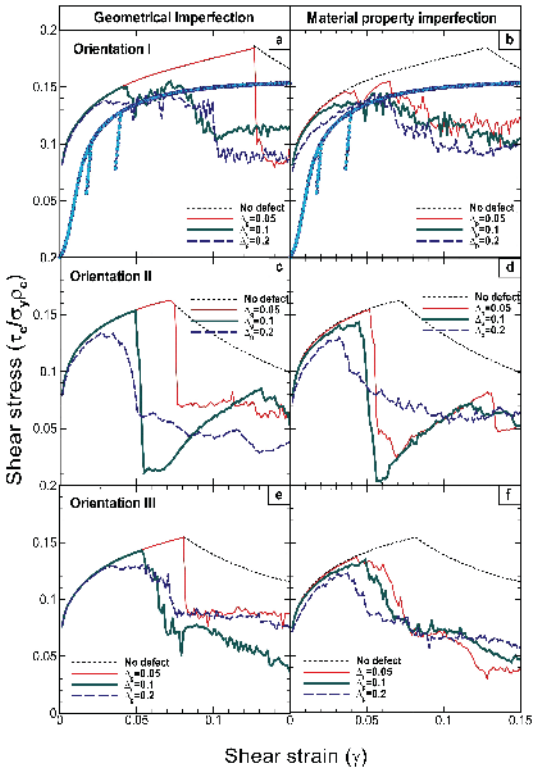

Fig. 8. Stress vs strain curves for the WBK truss models with defects. The curves show the different defect sensitivities on the shear directions (orientations I, II, III).

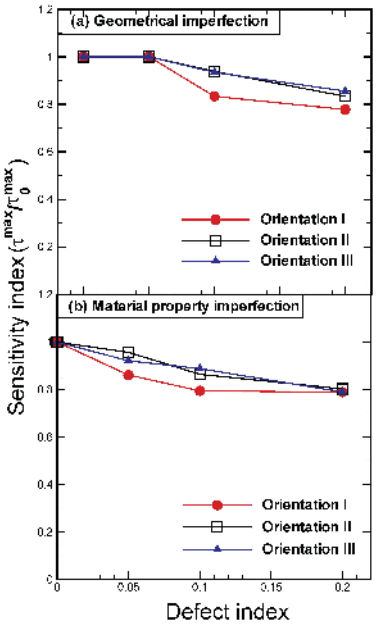

Fig. 9. The peak stresses vs defect index (standard deviations of the Gaussian imperfections of geometry and material property).

tations (II, III).

Fig. 9 shows the sensitivity curves of the maximum stress as a function of imperfection levels (Δ_g, Δ_p), for the three shear orientations. All the peak stresses of the defect models with geometric and material imperfections gradually decrease when the defect levels increase. However, no rapid drop of maximum stresses was observed as the imperfection levels increased, demonstrating the WBK can be robust to the imperfections.

The figure also shows relatively good isotropic characteristics (defect sensitivity as well as material strength) of the realistic WBK core under shear deformations, which is a prominent advantage of the WBK as a structural material.

5. Conclusions

This paper addressed the shear characteristics of the WBK structures and defect sensitivities of strengths, by using random network analysis incorporated with the finite element analysis. We summarize the conclusions as follows.

(1) The WBK under shear loads in the specified three orientations generally shows similar stress/strain behaviors in pre-yield regimes and similar maximum stresses.

(2) The simulation result for shear orientation I shows good agreement with the experimental measurement. It is suggested that the actual specimen may possess some degrees of geometric and material property defects generated in the fabrication process.

(3) The result from shear orientation I shows the highest maximum stress compared to the other orientations (II and III). It is relatively robust in the post-yield regime, too. In contrast, shear orientation II shows significant stress drops in the post-yield regime compared to other orientations.

(4) Before reaching the maximum stresses, no substantial effects of the imperfection were observed. However, as the geometrical and material imperfections increased, the strengths decreased slightly beyond the peak values.

Acknowledgment

This work was supported by the Korea Science and Engineering Foundation (KOSEF) grant funded by the Korea government (MOST) (R0A-2006-000-10249-0 & R01-2006-000-10349-0). One of the authors (S.H.) is also thankful for the financial support from the Korea Research Foundation Grant (MOEHRD: KRF-2005-042-C00037).

References

[1] S. Hyun, A. M. Karlsson, S. Torquato and A. G. Evans, Simulated properties of Kagome and tetragonal truss core panel, *Int. J. Solids Structures*, 40 (2003) 6989-6998.

[2] F. W. Zok, S. A. Waltner, Z. Wei, H. J. Rathbun, R. M. McMeeking and A. G. Evans, A protocol for characterizing the structural performance of metallic sandwich panels: application to pyramidal truss cores, *Int. J. Solids Structures*, 41 (2004) 6249-6271.

[3] D. J. Sypeck and H. N. G. Wadley, Cellular metal truss core sandwich structures, Banhart, J., Ashby, M.F., Fleck, N.A. (Eds), *Proc. of Cellular Metals and Metal Foaming Technology*, (2001) 381-386.

[4] V. S. Deshpande, N. A. Fleck and M. F. Ashby, Effective properties of the octet-truss lattice material, *J. Mech. Phys. Solids*, 49 (2001)1747-1769.

[5] S. Chiras, D. R. Mumm, N. Wicks, A. G. Evans, J. W. Hutchinson, K. Dharamasena, H. N. G. Wadley and S. Fichter, The structural performance of near-optimized truss core panels, *Int. J. Solids Structures*, 39 (2002) 4093-4115.

[6] H. N. G. Wadley, N. A. Fleck and A. G. Evans, Fabrication and structural performance of periodic cellular metal sandwich structures, *Composite Science and Technology*, 63 (2003) 2331-2343.

[7] A. G. Evans, J. W. Hutchinson, N. A. Fleck, M. F. Ashby and H. N. G. Wadley, The topological design of multifunctional cellular metals, *Prog. Mater. Sci.*, 46 (2001) 309-327.

[8] K. J. Kang, G. P. Jeon, S. J. Nah, B. S. Ju and N. H. Hong, A new way to manufacture ultra light metal structures, *J. Korean Soc. Mech. Eng. A*, 28 (2004) 296-303.

[9] Y. H. Lee, B. K. Lee, I. Jeon and K. J. Kang, Wire-woven bulk Kagome (WBK) truss cores, *Acta Material*, 55 (2007) 6084-6094.

[10] K. J. Kang and Y. H. Lee, Three-dimensional cellular light structures directly woven by continuous wires and the manufacturing method of the same, *Patent Pending*, PCT/KR2004/002864 /05 November (2004).

[11] Y. H. Lee, J. E. Choi and K. J. Kang, A new periodic cellular metal with Kagome trusses and its performance, *ASME International Mechanical Engi-*

neering Congress and Exposition, Chicago, USA, (2006) IMECE2006-15467.

[12] S. Hyun, J. E. Choi and K. J. Kang, Mechanical behaviors under compression in wire-woven bulk Kagome truss PCMs –Part I : Upper bound solution with uniform deformation, *Trans. of the KSME A*, 31(2007) 694-700.

[13] S. Hyun, J. E. Choi and K. J. Kang, Mechanical behaviors under compression in wire-woven bulk Kagome truss PCMs – Part II: Effects of geometric and material imperfections, *Trans. of the KSME A,* 31 (2007) 792-799.

[14] H. He and M.F. Thorpe, Elastic properties of glasses, *Phys. Rev. Lett.*, 54 (1985) 2107.

[15] D. J. Jacobs and M. F. Thorpe, Generic rigidity percolation: the pebble game, *Phys. Rev. Lett.*, 75 (1995) 4051.

[16] American Society for Testing and Materials Designation C273/C 273M, Standard Test Method for Shear Properties of Sandwich Core Materials, *Copyright ASTM International*, West Conshohocken, PA 19428-2959, United States.

[17] N. J. Mills, The high strain mechanical response of the wet Kelvin model for open-cell foams. *Int. J. Solids Structures*, 44 (2007) 51-65.

Sangil Hyun received his B.S. and M.S. degrees in physics from Seoul National University, Korea, in 1986 and 1989. He received his Ph.D. degree in solid state theory from Michigan State Uni-versity in 1998. Dr. Hyun is currently a senior researcher at the simulation center in Korea Inst. of Ceramic Eng. & Tech. (KICET). He is mainly working on computational studies on multifunctional cha-racteristics of fine ceramics, metals, and composites. He also develops a multiscale modeling on nanotribology and nanofluidics.

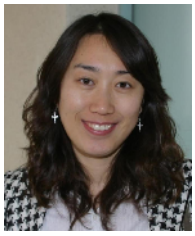

Ji-Eun Choi received her B.S. and M.S degrees in Mechanical Engineering from Chosun University, Korea, in 1999 and 2001. Ms. Choi is currently an associate research engineer at the automobile research center in Chonnam National University. She is mainly working on the theoretical and numerical analyses on truss PCMs (Periodic Cellular Metals).

Ki-Ju Kang received his B.S. degree in Mechanical Engineering from Chonnam National University, Korea, in 1981. He then received his M.S. and Ph.D. degrees from Korea Advanced Institute of Science and Technology in 1983 and 1988, respectively. Dr. Kang is currently a Professor at the School of Mechanical Systems Engineering at Chonnam National University in Gwangju, Korea. Prof. Kang's lab is designated as a national research Lab. His research interests include the optimal designs and manufacturing technologies of various types of porous cellular metals and mechanical behaviors of a thermally grown oxide at high temperature.